Latin American Journal of Solids and Structures
www.lajss.org

Analysis of sensor placement in beams for crack identification

Abstract
A previous study has shown that the mode shapes of a beam are more sensitive to damage than other vibrational parameters, thus making them better suited for crack identification purposes. However, they have the disadvantage of being more difficult to be measured. To overcome this difficulty, an interesting idea is to monitor changes produced by cracks on the mode shapes only in a few strategic points, instead of performing a complete experimental modal analysis. Considering this possibility, the aim of the present work was to determine the most appropriate locations for installing sensors in beams in order to identify and characterize structural damages. The effect of different locations of cracks on the mode shapes of beams was studied through a numerical (computational) model using the finite element model. The results were plotted in 3D graphs relating the relative nodal displacement of damaged and intact beams with the crack position and the location of the point analyzed. Through the analysis of these graphs, it was possible to point out the most adequate sites for placing sensors aiming at identifying cracks in a beam in fixed-free and fixed-fixed boundary conditions. Aiming at testing the results, an optimization problem for crack identification was proposed and solved through genetic algorithm (GA). The cracks were identified with an accuracy that is appropriate for engineering applications, showing that the proposed method is effective and could be used in Structural Health Monitoring (SHM) issues. Limitations on its use were also discussed.

Keywords
Structural Health Monitoring (SHM), modal analysis, crack identification, genetic algorithm (GA)

Marcus Vinícius M. Oliveira Filho[a*]
Juan Elías Perez Ipiña[b]
Carlos Alberto Bavastri[a]

[a] Universidade Federal do Paraná – UFPR, Curitiba, PR, Brazil. E-mail: marcus.oliveira.filho@gmail.com, bavastri@ufpr.br

[b] Universidad Nacional del Comahue – UNComa, Neuquén, Argentine. E-mail: juan.perezipina@fain.uncoma.edu.ar

*Corresponding author

https://doi.org/10.1590/1679-78254239

Received July 10, 2017
In revised form April 17, 2018
Accepted March 10, 2018
Available online April 04, 2018

1 INTRODUCTION

A marked improvement in computational tools and an increased commitment of researchers worldwide have contributed significantly to produce great advances in the areas of Damage Prognosis (DP) and Structural Health Monitoring (SHM) in recent years. Such advances have allowed an increase in system security and a reduction in the operational costs of various industrial processes and activities. One of the most important steps for the successful implementation of these techniques is the identification and characterization of cracks found in structures.

The presence of cracks induces local flexibility in structural elements, changing the vibration responses (Dimarogonas (1996)). The literature refers to these vibrational changes provoked by cracks as the "forward problem". It is possible, however, to determine the location and size of a crack observing such changes, which are referred to as the "inverse problem" (Rizos et al. (1990)). In general, damage detection methods consist in comparing the vibrational responses or the modal parameters of damaged structures to responses of intact structures and – by observing variations, numerical models, and optimization problems – in identifying the existence, location, and size of cracks. Beams, which are structures widely used in machinery, construction, mechanical engineering, shipbuilding, aviation industry, etc., are naturally among the most studied elements. Various researchers have analyzed changes among natural frequencies, vibration modes, and frequency response functions (FRF) of intact beams and cracked beams aiming at identifying damages (Fernández-Sáez et al. (1999), Douka et al. (2003), Owolabi et al. (2003), Hadjileontiadis et al. (2005), Loya et al. (2006), Al-Said (2007), Lee (2009), Srinivasarao et al. (2010), Attar (2012), Saeed et al. (2012), Gomes and Almeida (2014), Khiem and Tran (2014), Xu et al. (2014), Montanari et al. (2015), Fernández-Sáez et al. (2016), Zhang and Yan (2017)).

Analyzing those works, one notices that the monitoring of vibrational parameters is a feasible alternative for identifying cracks in beams. However, there is still no consensus about what technique would be the most recommended for each case, regarding the necessary precision, ease of measurement, and other factors. There are different alternatives in almost all steps of the crack identification process, among which one can highlight: the vibrational parameters to be analyzed and controlled, the physical approach to be adopted, the type and location of the sensor to be used, the numerical modeling, the optimization technique used, the quantification of errors and uncertainties, etc. Depending on the approach, some of those steps may be omitted, interconnected or unfolded. Finally, the combination of all those alternatives generate a wide range of available possibilities for identifying cracks in beams, each presenting its own advantages, disadvantages, and peculiarities. This range of options renders the process of selecting the most adequate method for each case very difficult as well as the decision on which approach to use when developing a new SHM or DP technique for a specific application.

Regarding the vibrational parameter to be analyzed, one can observe that the effect of cracks on natural frequencies has been significantly more studied than the effect of cracks on vibrating modes and on FRF, as, for instance, in the works of Fernández-Sáez and Navarro (2002), Lee (2009), Mazanoglu and Sabuncu (2012), Gillich and Praisach (2014), Moezi et al. (2015), Fernández-Sáez et al. (2016), Mungla et al. (2016), Eroglu and Tufecki (2016) and Zhang and Yan (2017). On the other hand, it is widely known that variations of natural frequencies of damaged beams are subtle even when the cracks are comparatively large – it is common for cracks whose depth is 30% of beam height to cause changes below 2% on the values of the natural frequencies (Owolabi et al. (2003), Mazanoglu and Sabuncu (2012), Gillich and Praisach (2014)). Very often, errors arising from the measurement system used have a higher magnitude than the variation of the natural frequencies produced by cracks, which makes it difficult to identify them. Likewise, numerical and computational models used in analyses and prognoses can also introduce unacceptable errors due to the high precision required in those applications.

Therefore, despite the difficulty in identifying small cracks through monitoring natural frequencies, from a technological point of view it is desirable to identify cracks when they are still at their initial stages. This is explained by the fact that larger cracks may already have compromised the structure as a whole or they may be identified through a simple visual inspection.

Motivated by these considerations, a previous work investigated the variations produced by different cracks on the natural frequencies, mode shapes, and FRF of a cantilever beam numerically, through the finite element method (Oliveira Filho et al. (2017)). It is significant to point out that even small cracks ($a/h = 0.1$) produced significant changes on the vibration mode of the beam. In the third mode, for example, this crack size produces changes of 5% over the values of the vertical displacements of nodes, when compared to intact beams; in the fourth mode, the changes were above 3%. It was found out that the vibration modes are more sensitive than both natural frequencies and the FRF of beams for a damage of the same magnitude.

In that occasion, the relative vertical displacements (the percent relation between the nodal displacement of damaged and intact beams) of the first five mode shapes were observed in ten equally spaced nodes, for 28 different damage scenarios. The results were presented in 3D graphs relating the relative nodal displacement RND with crack position and the node analyzed, showing that some sites are more damage sensitive than others. Since these sites amplify the effects caused by damage on the vibrational behavior of the structure, they are more appropriate for sensor placement for crack identification purposes.

Previous studies found in the literature have already investigated the effects caused by cracks on beam mode shapes, and have also solved the inverse problem by monitoring this parameter. Rizos et al. (1990) monitored the vibrating modes of cracked cantilever beams, identifying cracks with reasonable accuracy when they had moderate depths – above 10% of the beam height. Douka et al. (2003) presented a simple method of identifying cracks in cantilever beams based on an analysis of the fundamental vibration mode of the structure and on intensity factors that allow estimating the severity of the damage. Hadjileontiadis et al. (2005) analyzed the fundamental vibration mode of a cantilever beam to propose a technique for identifying cracks, which proved to be able to detect the damage even in the presence of noises in the analyzed signal. In order to solve the inverse problem, Lu et al. (2013) used a method that was insensitive to measurement noise, based on the difference between the curvature of the vibration modes of damaged and intact beams. Khiem and Tran (2014) obtained a simplified expression for the natural vibration modes of a beam with an arbitrary number of cracks and, even with noisy and scarce data, the researchers managed to perform damage identification. Xu et al. (2014) proposed two methods based on the measurement of the vibration modes of cracked beams, which allow identifying damage without the prior need to have information about the beams in their intact condition. Montanari et al. (2015) simulated numerically the first three vibration modes in cantilever beams and on simply supported beams, and used the results to determine the optimal number of sampling intervals to identify the damage in an effective way.

Despite the relevant advances obtained in recent years in monitoring mode shapes of beams as the core point for solving the inverse problem, an inconvenient issue persists. There are two available options to obtain the mode shapes experimentally: it is necessary either to excite the whole structure with an impact hammer or to place sensors on the entire structure, and excite it either with a shaker or in an operational way. The problem regarding the first option is that it demands a specialist to test the structure *in situ*, which impairs the use of this type of technology for remote applications, or when the structures to be monitored are numerous. The problem regarding the second options is that it may become too expensive. In the light of these considerations, it is reasonable to think about monitoring the beam by placing sensors in only a few strategic points as a feasible way to detect the damage, since it avoids the two problems pointed out previously. In addition, techniques for adopting an appropriate sensing for SHM issues constitute a recurrent topic discussed in the literature, as highlighted in the works of Khavita et al. (2016) and Kanaparthi et al. (2016).

This way, the objective of the present study is to determine the most appropriate sites for placing sensors in beams for crack identification purposes, by monitoring the mode shapes of the structure. The present work adds to the previous study by observing the RND in more points, leading to more accurate 3D charts about beam sensitiveness to damage. In addition, the simulations were replicated for the fixed-fixed beam condition. Aiming at testing the results, a crack identification problem was proposed and solved with the aid of the genetic algorithm (GA). The results are shown in section 3.

2 METHODOLOGY

In order to obtain data from vibrational responses, a computational model of the beam was created using the finite element method, following the approach of various works found in the literature (Krawczuk (1992), Owolabi et al. (2003), Sankararaman et al. (2011), Mazanoglu and Sabuncu (2012), Amitt et al. (2014), Xu et al. (2014), Simoen et al. (2015)). The following sections present details of the numerical model used and vibration responses obtained.

2.1 Numerical model

First, a model of an intact Euler-Bernoulli beam was created, crack free, using the commercial ANSYS software. This model contains information on the geometry and material of the structure and is necessary to determine the vibrational behavior of the structure before any damage appears. The beam under study has a square cross-section, parameterized with length L, width w, and height h. The material considered was steel, with an elastic modulus $E = 206.8 GPa$, density $\rho = 7830\, kg/m^3$, and Poisson coefficient $\nu = 0.33$. The finite element mesh was created considering the longitudinal middle of the intact beam, using 10000 square solid elements of 8 nodes. The average element size was set to $L/1000$. The beam was studied with two different boundary conditions: fixed-free (cantilever) and fixed-fixed.

In order to make sure that the numerical model was calibrated, the first five natural frequencies (f_n) were obtained numerically and compared to the natural frequencies calculated through the analytical equation below (Blevins (1979)):

$$f_n = \frac{\lambda_n^2}{2\pi L^2}\sqrt{\frac{EI}{m}} \tag{1}$$

where E is the elastic modulus of the material, I is the inertia moment of area about neutral axis, m is the mass per unit length of beam and λ_n is a constant coefficient which depends on the boundary condition and on the n^{th} natural frequency of the beam.

It is worth pointing out that the calculation of natural frequencies and mode shapes leads to the same results for a fixed-fixed and a free-free boundary condition. The last one is commonly adopted when performing an experimental modal analysis. For $L = 1m$, $w = 0.010m$ and $h = 0.010m$, the obtained results are presented in Table 1:

Table 1: *Comparison between the analytical natural frequencies and those of the numerical model.*

Natural frequency	Finite element method (Hz)	Analytical solution (Hz)	Difference (%)
Fixed-free boundary condition			
f_1	8.30	8.30	0.00
f_2	52.01	52.03	-0.04
f_3	145.51	145.68	-0.12
f_4	284.82	285.47	-0.23
f_5	470.15	471.90	-0.37
Fixed-fixed boundary condition			
f_1	52.81	52.83	-0.04
f_2	145.43	145.62	-0.13
f_3	284.75	285.47	-0.25
f_4	469.98	471.90	-0.41
f_5	700.76	704.94	-0.59

Analyzing the table, it is possible to observe that the percentage difference between the model used and the analytical solution had an average of –0.218% and did not exceed 0.6% (absolute value) in any of the frequencies, thus indicating that the model is adequate.

Then, cracks were inserted into the numerical model. As the simulation of cracked structures requires mesh alterations depending on crack position and depth, the mesh of the longitudinal sections of the structures with cracks contained about 1008 square elements of 8 nodes. This number may present small variations depending on the crack parameters. Although it is common to use singular elements to model the crack tip, this type of modeling is recommended when one intends to calculate stresses and strains in the crack vicinity. When global variations on the dynamic behavior of the structure are intended to be calculated, this specific type of modeling is unnecessary, besides presenting the drawback of increasing the computational cost (Chati et al. (1997)). Therefore, the same 8-node square elements were used in the entire model. Figure 1 illustrates the mesh of finite elements used in the crack tip area.

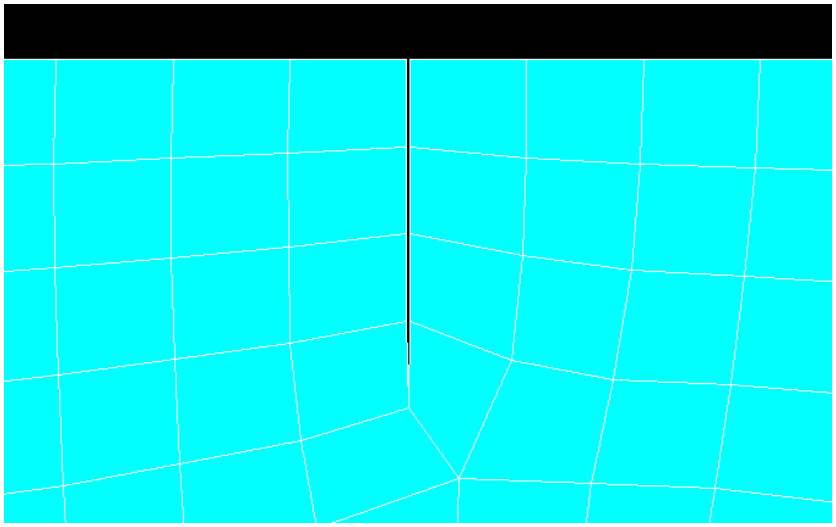

Figure 1: *Finite element mesh in the crack tip area.*

The crack location xc varied in the model. The crack depth a was kept constant in all simulations ($a/h = 0.3$), because it was previously observed that this parameter does not change the pattern of the 3D graphs relating RND with crack position and the node analyzed (Oliveira Filho et al. (2017)). As a matter of fact, crack depth only changes the amplitudes of the curves: the deeper the crack, the bigger the RND observed, but the curves shapes are kept the same. Therefore, since the objective of the present study is to determine the most

appropriate sites for installing sensors in beams, only the curves shapes need to be observed, which justifies the choice of keeping the crack depth constant.

The shape of the crack and its width were defined based on the height of the beam, according to the schematic drawing in Figure 2, illustrating the fixed-free boundary condition.

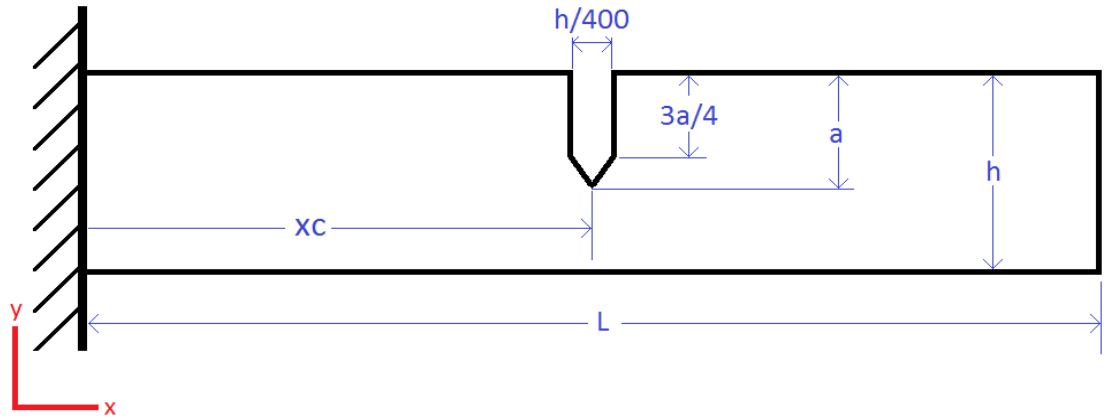

Figure 2: *Sketch of beam format and width – not in scale.*

During simulations, different crack positions xc_i were considered for both studied boundary conditions, where i ranges from $1 \leq i \leq 19$ and represents the crack position as in Table 2. On the whole, 38 different scenarios (19 for the fixed-free case and 19 for the fixed-fixed case) were analyzed.

Table 2: *Positions of cracks under study.*

Crack position (xc / L)	
xc_1	0.05
xc_2	0.10
xc_3	0.15
xc_4	0.20
xc_5	0.25
xc_6	0.30
xc_7	0.35
xc_8	0.40
xc_9	0.45
xc_{10}	0.50
xc_{11}	0.55
xc_{12}	0.60
xc_{13}	0.65
xc_{14}	0.70
xc_{15}	0.75
xc_{16}	0.80
xc_{17}	0.85
xc_{18}	0.90
xc_{19}	0.95

2.2 Vibration responses

For each of the 38 scenarios, a modal analysis was performed. The same analyses were performed for the crackless beam situations.

Through modal analysis, the first 5 natural frequencies and the beam associated vibration modes were extracted for each scenario. The vertical nodal displacements of the cracked beam uc_j of 21 different sites in the beam were were monitored, located at $x = 0$ (with increments of $L/20$ until total length L), height $y/h = 0.1$ and width $z/w = 0.5$. Such choice was made to make sure that the sites under study were always located in the remaining ligament of the beam. The index j ranges from $1 \leq j \leq 21$, denoting the site under study.

These uc_j values were calculated using the Block Lanczos algorithm available in the ANSYS software, and the results were normalized by the mass matrix. Since these nodal displacements are used for a proportional calculation (se eq. (2) for more details), there would be no difference were the results normalized to the unity or unnormalized.

All the analyses were performed for both boundary conditions. By definition, uc_1 and uc_{21} equal zero for the fixed-fixed boundary condition. In the fixed-free case, only uc_1 renders null. Figures 3 and 4 present a schematic view of the side and front views of the beam for the two cases, showing all the sites under study.

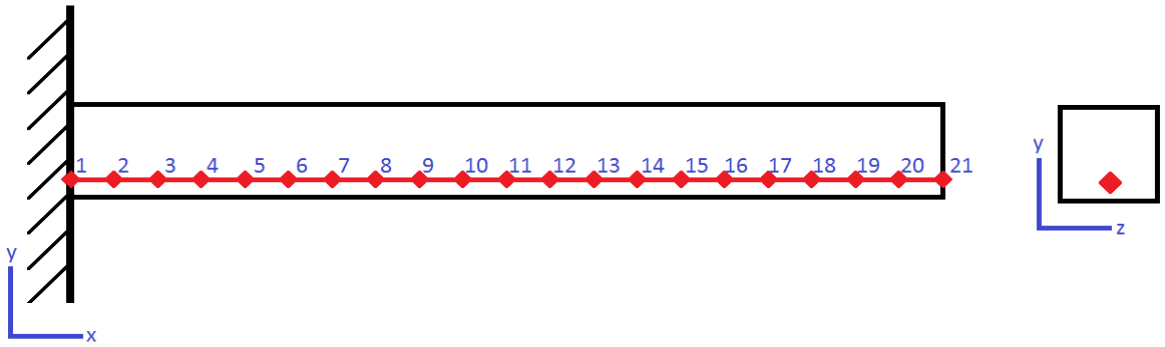

Figure 3: *Side and front views of the fixed-free beam showing the 21 sites under study.*

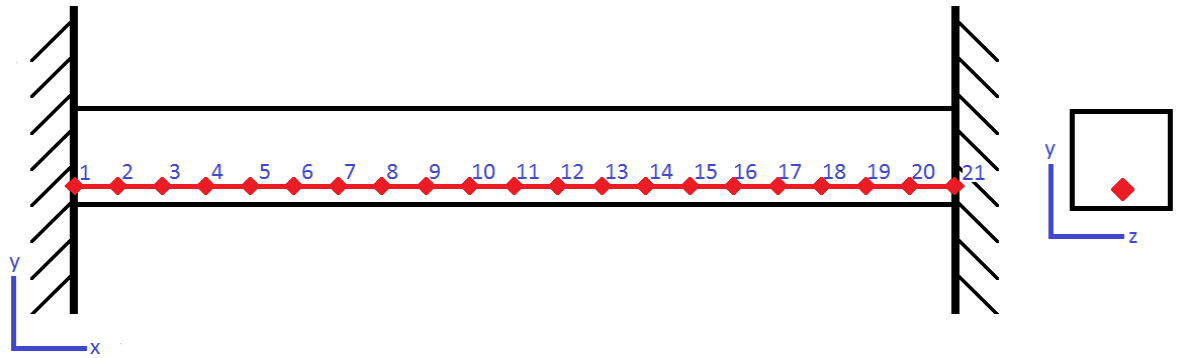

Figure 4: *Side and front views of the fixed-fixed beam showing the 21 sites under study.*

The vertical nodal displacements for the intact beam ui_j were also calculated, following the same methodology presented for the uc_j. Then, it was possible to determine the relative nodal displacement RND_j for each studied point. This parameter is the percentage variation of the nodal displacement regarding the cracked and the intact beam cases, given by:

$$RND_j = 100\left(\frac{uc_j - ui_j}{ui_j}\right) \tag{2}$$

For each crack introduced into the model, the RND_j gives a single shift pattern of each mode shape of the beam. This shift pattern can be used to solve the inverse problem, i.e., to determine which crack position and depth produced the observed variations in the mode shapes.

2.3 Relative nodal displacement 3D graphs

Since each one of the calculated relative nodal displacements depends on two parameters – crack position and the position of the node under study –, their values were stored in matrices of dimensions $i \times j$, where i is the position of the crack and j is the position of the node. Then, it was possible to plot 3D graphs relating the RND with the crack position xc/L and the position of the node analyzed x/L, which made it easier to visualize the results. Based on these graphs, one can visually observe the nodes in which the maximum RND amplitudes are developed, regardless the crack position, i.e., the positions which are more sensitive to the damage. These positions are the most appropriate for installing sensors onto the beam, because they amplify the damage effects on the structure mode shapes, making the process of solving of the inverse problem easier and less susceptible to possible numerical and experimental errors. The graphs obtained are displayed in section 3.

2.4 Optimization problem

Aiming at testing the results that were found numerically, an optimization problem for solving the inverse problem of identifying the crack was proposed. First, a crack with known position and depth was introduced numerically into the model, and the RNDs were calculated for it. This step could be substituted by an experimental setup in future works, where the cracks could be introduced in real beams.

Although the entire RND matrix can be calculated for the introduced crack, only the columns related to the places where the sensors would be installed were used. For instance, if one places three accelerometers into the beam, located at $x/L = 0.10$, $x/L = 0.50$ and $x/L = 0.80$ ($j = 3$, $j = 11$ and $j = 17$, respectively), only vectors RND_3, RND_{11}, and RND_{17} would be available. The choice of position for the sensor should take into account the sensitivity of the different mode shapes of the beam in that point regarding the crack parameters, a and xc. So, continuing with the example, one could use the sensor placed at $x/L = 0.10$ to monitor the changes in the first mode shape, the sensor placed at $x/L = 0.50$ to monitor the changes in the third and fifth mode shape, and the sensor placed at $x/L = 0.80$ to monitor the changes in the second mode shape. This way, four different values of the relative nodal displacements would be used to configure the shift pattern that a crack produced on the mode shapes of the structure. The choices of these values should be made based on the 3D charts presented in Oliveira Filho et al. (2017) and in sections 3.1 and 3.2.

These values can be stored in a vector of dimension l, called reference curve RC, given by:

$$RC_{(l)} = \left[RND_{j,k} \right] \tag{3}$$

where l is the number of elements used to configure the shift pattern, j is the position of the sensor installed, and k is the mode shape monitored. In the given example, the reference curve used would be given as:

$$RC_{(4)} = \left[RND_{3,1}\ RND_{11,3}\ RND_{11,5}\ RND_{17,2} \right] \tag{4}$$

Knowing the reference curve obtained for a crack, one can propose an optimization problem that simulates the effect of a different combination of crack position and depth in the beam mode shapes in each iteration. Then, the RND can be calculated for each crack as in eq. (2), and the monitored values (naturally, the same positions and mode shapes used for the reference curve) are stored in another vector of dimension l, called numerical curve NC.

Finally, an objective function S is used in order to minimize the difference between the RND obtained for the reference curve and the numerical curve. The objective function also includes a weighting coefficient w to normalize the elements in the same scale, as follows:

$$S = \sum_{m=1}^{l} \frac{\sqrt{\left(RC_m - NC_m \right)^2}}{w_m} \tag{5}$$

where l is the number of elements used. The weighting coefficient w depends on the mode shape monitored, and is given by the maximum absolute value obtained in the 3D graph for that mode. If one uses a different crack size to generate these graphs ($a/h = 0.5$, for example), although the weighting coefficients found would be different from the ones of the present situation, it would have no impact for the crack identification problem, since the values of w would be altered in a proportional way.

Restrictions were imposed for the crack position and depth, as follows:

$$0.01 \leq xc/L \leq 0.99 \tag{6}$$

$$0.004 \leq a/h \leq 0.8 \tag{7}$$

2.5 Genetic algorithm

The genetic algorithm (GA) was used to solve the optimization problem. The algorithm is a non-linear method based in the natural evolution process, from Darwin's theory. Basically, an initial population – a set of individuals – of possible solutions is selected randomly through the search space. In this case, each individual is formed by two parameters: the crack position xc and the crack depth a. After the testing of this generation, the best-fitted individuals are kept for the next one (this process is usually called "elite count" or choosing the "champions"). The rest of the generation suffers from mutation and crossover, giving place to a new set of individuals that also compose the second generation. This process continues until a virtually best individual is found, i.e., a combination of crack position and depth whose RND agree the most with the ones obtained for the known crack. The number of individuals in each generation and the number of generations are pre-determined in the algorithm, and optimization stops when a minimum value of tolerance set to the objective function is reached, or when all individuals of all generations are tested.

The use of the GA to solve some kind of crack identification problem is already established in the literature, as in the works of Khaji and Mehrjoo (2014), Mehrjoo et al. (2014), Hou and Lu (2016), Mungla et al. (2016), and Eroglu and Tufecki (2016). This algorithm is convenient to this particular problem, since it does not use an initial candidate to start the optimization, but a family of them. The choice of a unique initial candidate for the optimization is an obstacle for solving the problem, since it increases the possibility of the solution converging to a local minimum – a false position and depth of the crack.

In other works, the initial population was selected as 15 times the number of variables, which leads to 30 individuals for two parameters – crack position and depth (Khaji and Mehrjoo (2014), Mehrjoo et al. (2014), Eroglu and Tufecki (2016)). However, this number was increased by 50% in the present work, leading to an initial population of 45 individuals. This decision was made to increase the probability of finding the global minimum of the function. The tolerance of the objective function was set to 10^{-6} , i.e., optimization stops when the S assumes a lower value than that. It was observed that the variations regarding crack depth and position when S assumes a lower a value than the established tolerance are negligible for crack identification purposes. The number of generations was set to 20, and the elite count was set to 3 individuals. The probability of crossover was set to 0.9.

In order to solve the optimization problem, a routine was developed in the MATLAB software. For each iteration, the software generates a text file called "parameters", which contains the crack parameters to be tested. In a further programming line, the ANSYS software is activated and starts to run in batch mode. The software ANSYS, at its turn, uses another pre-determined parameterized programming routine, and reads the file "parameters", earlier exported. After the simulations, software ANSYS exports its results in text files, which are read by MATLAB, allowing the optimization to continue. This process runs automatically, being a powerful and convenient alternative for solving the inverse problem.

3 RESULTS AND DISCUSSION

The following sections present the results obtained from the simulations related to variations perceived in vibration modes of the beam, for the two studied boundary conditions. The results of the optimization problem are also presented.

3.1 Fixed-free boundary condition

Figures 5 to 9 present three-dimensional charts of the first 5 vibration modes for the fixed-free boundary condition, establishing a relationship among the crack position, the position of the analyzed node and the percentage variation between the nodal displacement of damaged beams and intact beams.

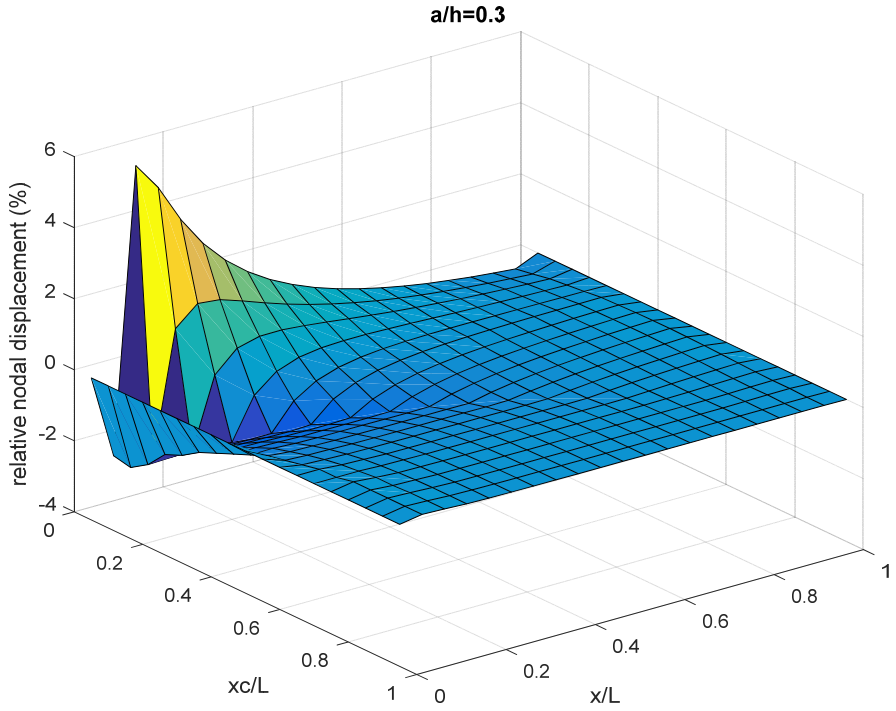

Figure 5: *Variations in the 1st vibration mode based on the crack and on the site under study.*

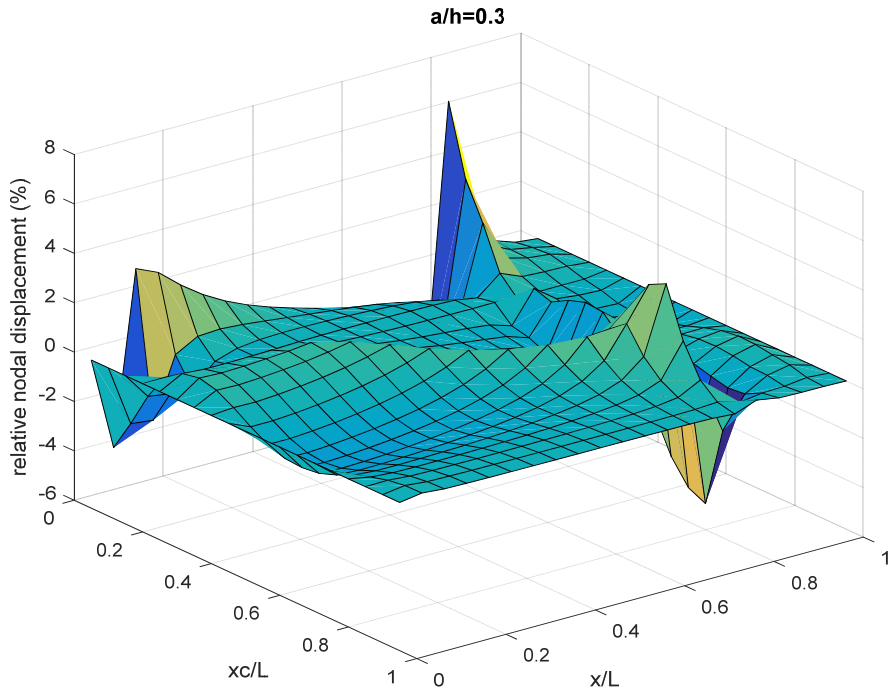

Figure 6: *Variations in the 2nd vibration mode based on the crack and on the site under study.*

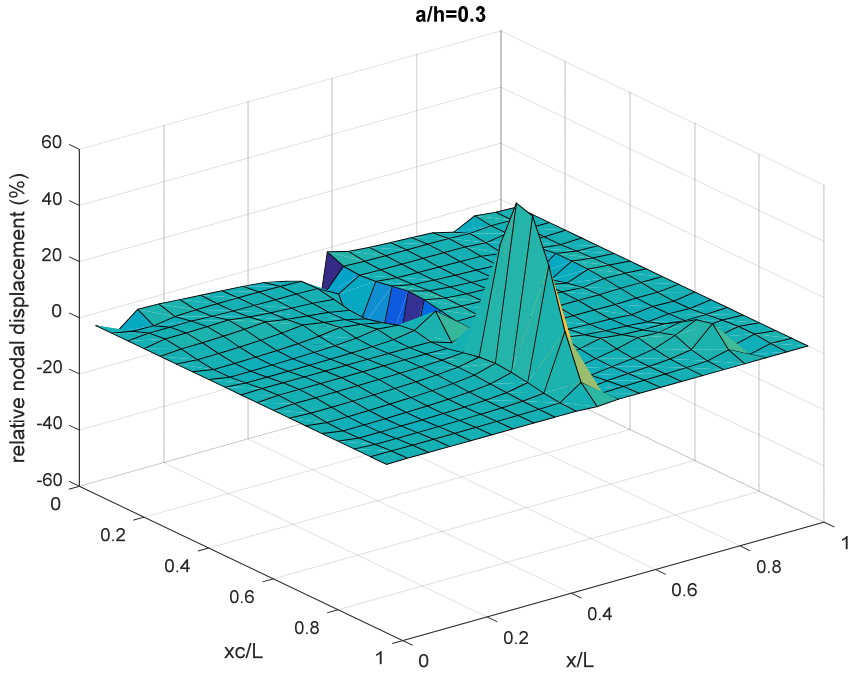

Figure 7: *Variations in the 3rd vibration mode based on the crack and on the site under study.*

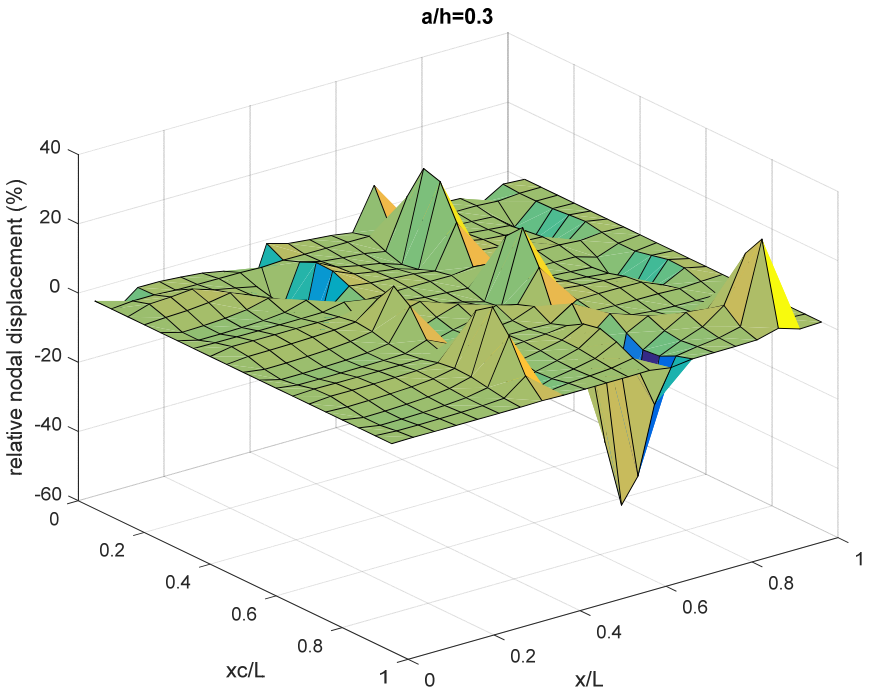

Figure 8: *Variations in the 4th vibration mode based on the crack and on the site under study.*

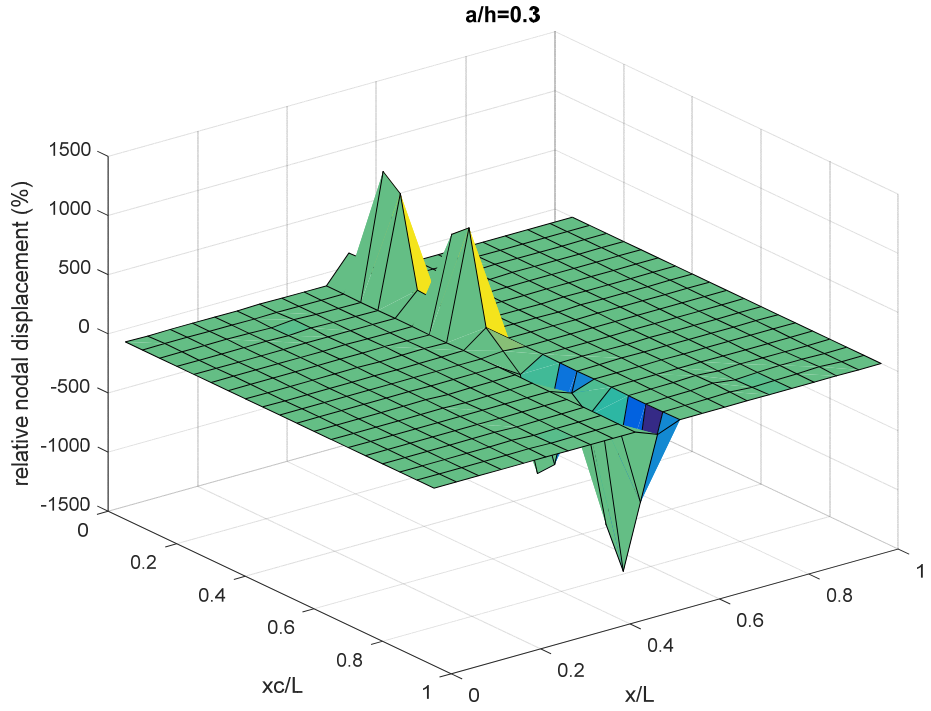

Figure 9: *Variations in the 5th vibration mode based on the crack and on the site under study.*

Analyzing those charts, it is possible to observe that the variation of the vertical displacement of nodes produced by cracks strongly depends on the position of x/L of the observed node, vibration mode and position of the crack. For the third and fifth vibration modes (Figures 7 and 9), for example, cracks produced significant variations in the vertical displacement of nodes located in the middle section of the beam, that is, $x/L=0.5$. For the first vibration mode (Figure 5), the most significant variations are observed in the nodes located at $x/L=0.1$. For the second vibration mode (Figure 6), the effect is more pronounced at $x/L=0.8$ and, for the fourth vibration mode (Figure 8), the effects are more pronounced at $x/L=0.35$, $x/L=0.65$, and $x/L=0.9$.

Based on the calculated results, the weighting coefficients W of each mode were also obtained for the fixed-free boundary condition, as in Table 3:

Table 3: *Weighting coefficients for the fixed-free boundary condition.*

Mode shape	Weighting coefficient W
1	5.6201
2	6.5399
3	58.2674
4	47.4693
5	1366.5

3.2 Fixed-fixed boundary condition

Similarly, Figures 10 to 14 present three-dimensional charts of the first 5 vibration modes for the fixed-fixed boundary condition.

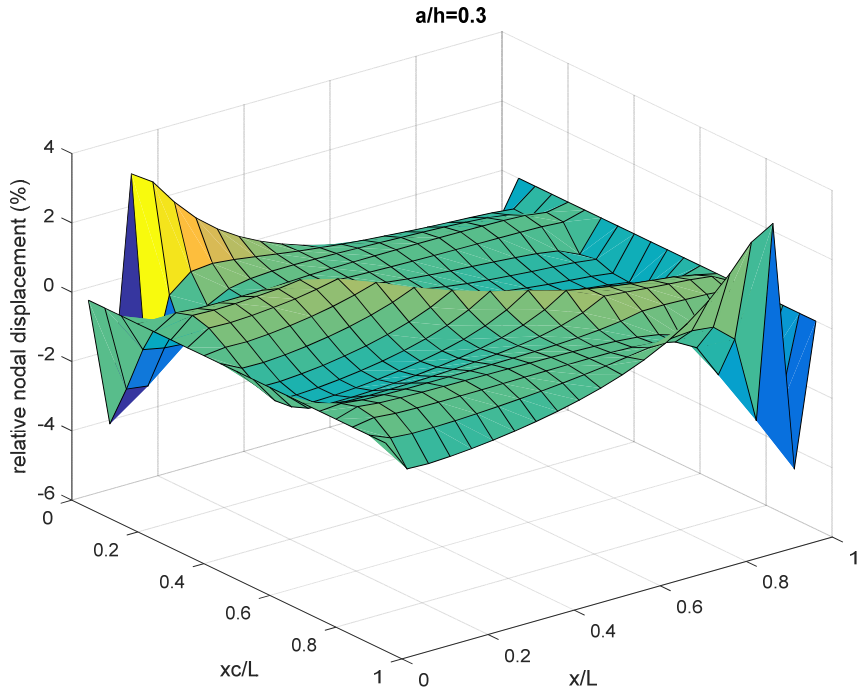

Figure 10: *Variations in the 1st vibration mode based on the crack and on the site under study.*

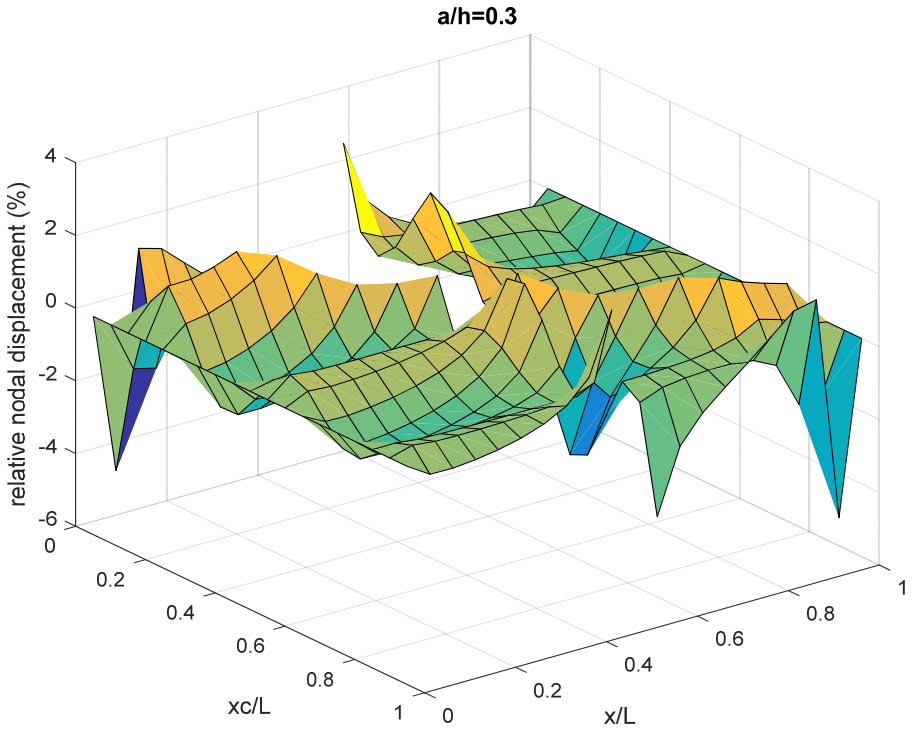

Figure 11: *Variations in the 2nd vibration mode based on the crack and on the site under study.*

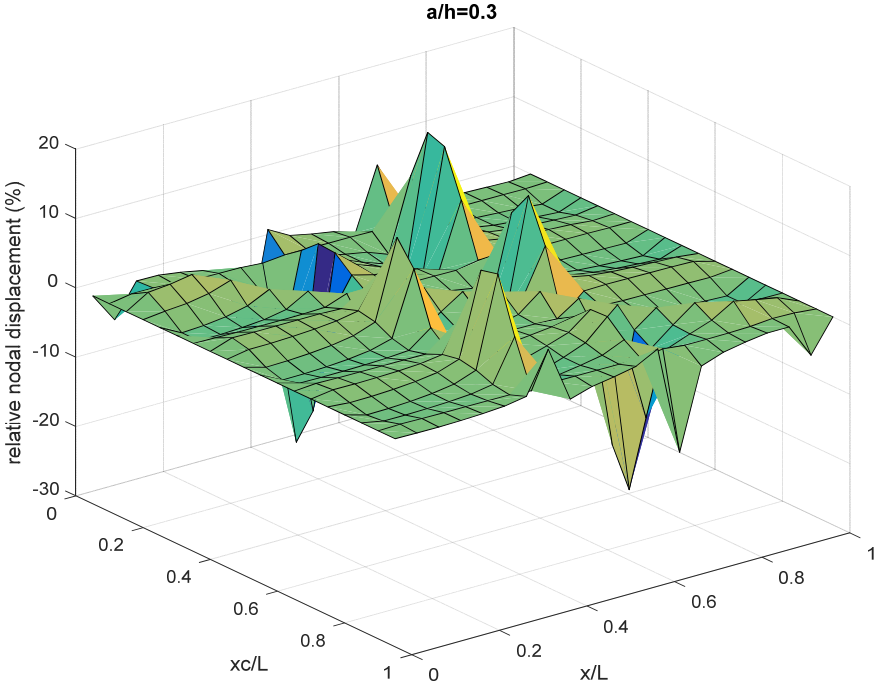

Figure 12: *Variations in the 3rd vibration mode based on the crack and on the site under study.*

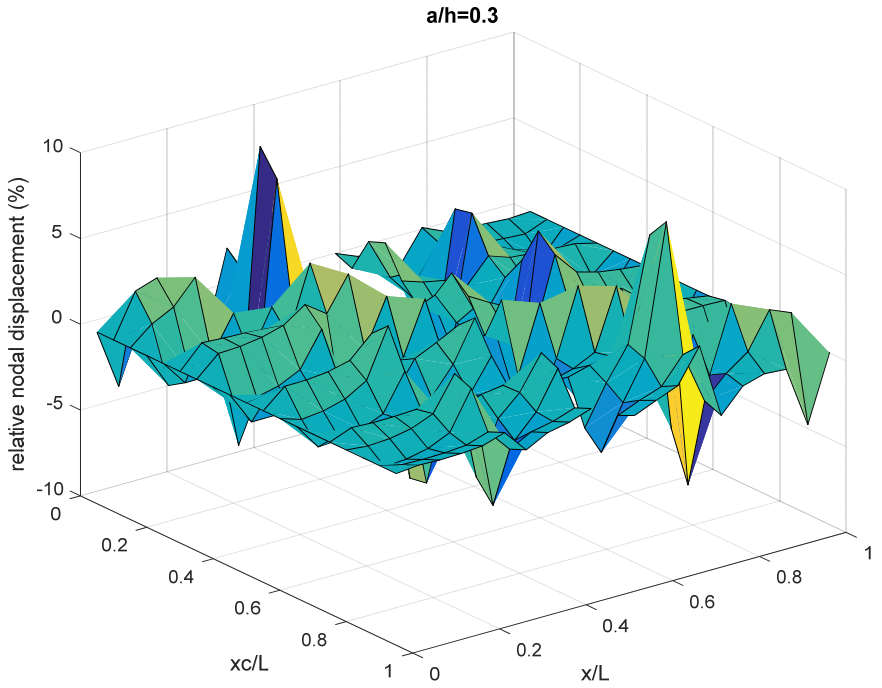

Figure 13: *Variations in the 4th vibration mode based on the crack and on the site under study.*

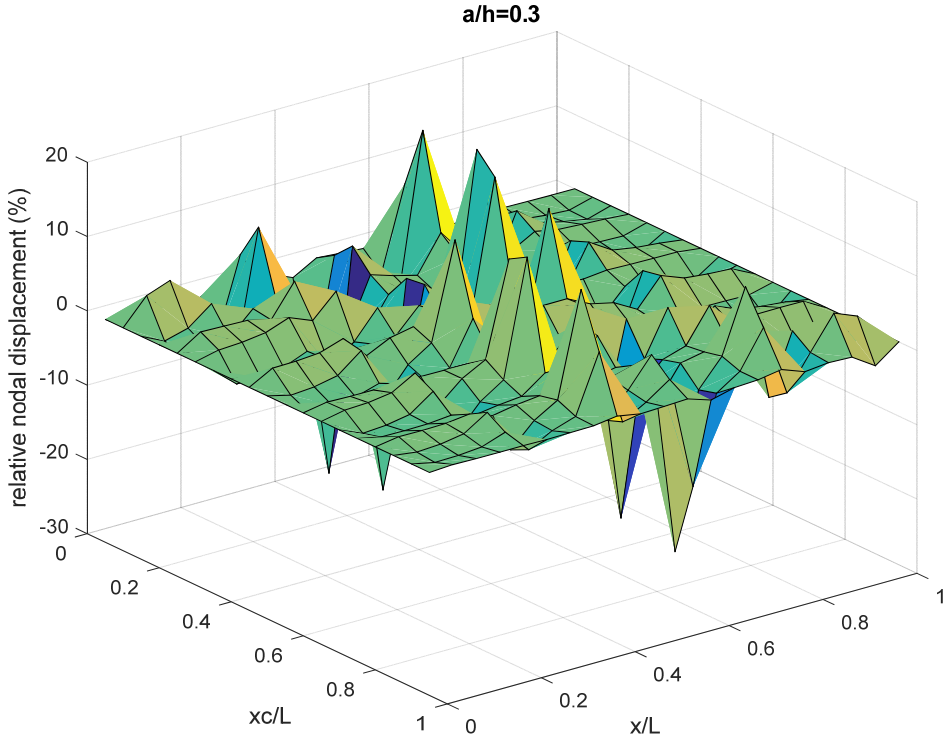

Figure 14: *Variations in the 5th vibration mode based on the crack and on the site under study.*

Once again, the variation of the vertical displacement of nodes produced by cracks depends on the position of x/L. Because of the symmetry of the boundary condition (fixed-fixed), a symmetry is also observed in the 3D charts for these situations. The positions that are more sensitive to damage can be estimated by the graphs for each mode shape; in this boundary condition, they appear in the coordinates x and $L-x$. For the first vibration mode, cracks produced significant variations at $x/L=0.1$ and $x/L=0.9$; for the second vibration mode, at $x/L=0.05$, $x/L=0.45$, $x/L=0.55$ and $x/L=0.95$; for the third vibration mode, at $x/L=0.35$ and $x/L=0.65$; for the fourth vibration mode, at $x/L=0.25$, $x/L=0.30$, $x/L=0.70$ and $x/L=0.75$; for the fifth vibration mode, at $x/L=0.40$ and $x/L=0.60$.

For the second and fourth vibration modes, a discontinuity appears in the graphs in the middle point of the beam, $x/L=0.5$. This happens because, for the fixed-fixed boundary condition, the vertical displacement of these modes equals zero for the intact beam at this point. When eq. (2) is applied, a division by zero appears, which means that, at this point, the RND tends to infinite. Therefore, the use of these points for the referred mode shapes should be avoided for crack identification purposes, since it could lead to erroneous results, especially when considering an experimental setup.

Based on the calculated results, the weighting coefficients W of each mode were also obtained for the fixed-fixed boundary condition, as in Table 4:

Table 4: *Weighting coefficients for the fixed-fixed boundary condition.*

Mode shape	Weighting coefficient W
1	4.0876
2	4.7519
3	23.8350
4	9.6287
5	25.4554

3.3 Inverse problem

To test the effectiveness of placing sensors at the sensible positions pointed by the 3D graphs, different cracks were simulated in the numerical model. The RND they produced were used to solve the inverse problem, as described in section 2.4. The method was tested for the fixed-free boundary condition. Three points were used to control the changes that the cracks caused, by monitoring the variation of four RND, as in Table 5:

Table 5: *Monitored points.*

Point	Position	Mode shape monitored
1	$x/L = 0.1$	1st
2	$x/L = 0.5$	3rd and 5th
3	$x/L = 0.8$	2nd

Table 6 presents the positions and depths of the different cracks that were simulated, as well as the identified crack, according to the proposed optimization problem. The depths and positions of the simulated cracks were chosen arbitrarily, with the objective of preliminarily testing the efficacy of the method for cracks hypothetically spread throughout the whole beam.

Table 6: *Identified cracks and errors.*

Crack	Real crack parameters		Identified crack parameters		Error (%)	
	$a/h(\%)$	x/L	$a/h(\%)$	x/L	a/h	x/L
1	5.0	0.620	5.1	0.619	2.0	-0.16
2	10.0	0.300	10.9	0.307	9.0	2.33
3	20.0	0.160	19.3	0.164	-3.5	2.44
4	30.0	0.750	28.8	0.748	-4.0	-0.27
5	30.0	0.820	29.2	0.817	-2,7	-0.37

The results show that, by monitoring three points (which would demand the use of three sensors in an experimental setup), the proposed method was able to identify cracks with an acceptable precision for many engineering applications. It is worth pointing out that even small cracks ($a/h = 5\%$) were identified. This is possible because the changes produced by cracks of this size on the beam mode shapes are more significant than the ones observed on the natural frequencies and FRFs, as shown in the previous study.

It is relevant to notice that the present results were obtained through numerical simulation, which is different from a practical situation where experimental issues have to be considered. However, as a preliminary approach, the type and the characteristics of the used sensors should have little influence on the method's damage detection capacity, since the sensors would affect the vibrational behaviour of the beam before and after the crack appearance. Therefore, since the method is based on a relative comparison between the damaged and the intact scenarios (see eq. (2)), these sensors effects shall be attenuated. These issues could be investigated by future studies, aiming at testing the applicability of the proposed methodology in experimental setups, which always present further challenges due to the experimental errors involved.

Also, as in any crack identification technique, when considering a more realistic experimental case, it is clear that the variations observed in the RND could also be caused by other factors besides the appearance of a single crack, such as other cracks, ground accommodations and other structural changes. These effects present an additional difficulty in the damage identification task.

4 CONCLUSIONS

This study adds to the results found in a previous one, which pointed out that the mode shapes are more sensitive to cracks than the natural frequencies and the FRF of beams; it was also observed that the amplitude of the changes regarding those parameters is proportional to the size of the observed crack. Therefore, the effects of different crack positions on the mode shapes of fixed-free and fixed-fixed beams were studied using a computational numerical model.

Although the mode shapes have shown to be more sensitive to the damage than other parameters, and, consequently, better suited for crack identification, they have the disadvantage of being more difficult to be measured. To overcome this difficulty, the idea was to monitor the changes that cracks produce on the mode shapes only in a few strategic points, instead of performing a complete experimental modal analysis.

Aiming at determining which positions are more sensitive to damage, and, naturally, more appropriate for installing sensors, 3D graphs relating the relative nodal displacement with different crack positions and different studied sites were plotted. Considering all the different cracks, studied positions, mode shapes, and both boundary conditions, a total of 3990 points were evaluated. Based on these graphs, one can choose a combination of sites to place a set of sensors and monitor the changes in different mode shapes, thus aiming at solving the crack identification inverse problem. Using three accelerometers in the fixed-free beam, for example, it would be convenient to place them at $x/L=0.1$ (first vibration mode monitoring), $x/L=0.5$ (third and fifth vibration modes monitoring), and $x/L=0.8$ (second vibration mode monitoring). Depending on the vibration mode analyzed and the number of available sensors, one could think of other advantageous combinations.

Cracks were created in the computational model and an optimization problem based on the genetic algorithm was proposed and solved to test the information contained in the graphs. Analyzing the three points mentioned in the previous paragraph, the cracks were identified with an accuracy that is appropriate for engineering applications. Even small cracks ($a/h=5\%$) – referred to in the literature as being difficult to identify due to experimental and numerical errors – were properly characterized.

The results have shown that the proposed method is effective and could be used for SHM purposes. However, more studies must be carried out to determine the minimum number of sensors necessary to correctly identify a crack. When a number of sensors below the required value is used, there may exist more than one combination of crack depth and position that leads to the observed shift pattern on the beam mode shapes, i.e., an optimization problem with no unique solution. This could cause false cracks to be identified. Also, further studies could test the method experimentally, which is always a bigger challenge due to the experimental errors involved.

5 ACKNOWLEDGEMENTS

The authors thank the Human Resources Program 24 (PRH-24) of the National Petroleum Agency (ANP) of Brazil and the CNPq – Brazil's National Council for Scientific and Technological Development, for having granted the scholarship that allowed the present work to be developed.

References

Al-Said, S. M., (2007). Crack identification in a stepped beam carrying a rigid disk, Journal of Sound and Vibration 300:863-876.

Amitt, E., Givoli, D., Turkel, E., (2014). Time reversal for crack identification, Computational Mechanics 54:443-459.

Attar, M., (2012). A transfer matrix method for free vibration analysis and crack identification of stepped beams with multiple edge cracks and different boundary conditions, International Journal of Mechanical Sciences 57:19-33.

Blevins, R.D. (1979). Formulas for natural frequency and mode shape. Van Nestrand Reinhold Company, New York.

Chati, M., Rand, R., Mukherjee, S., (1997). Modal analysis of a cracked beam, Journal of Sound and Vibration 207:249-270.

Dimarogonas, A.D., (1996). Vibration of cracked structures: a state of art review, Engineering Fracture Mechanics, 55:831-857.

Douka, E., Loutridis, S., Trochidis, A., (2003). Crack identification in beams using wavelet analysis, International Journal of Solids and Structures 40:3557-3569.

Eroglu, U. and Tufecki, E., (2016). Exact solution based finite element formulation of cracked beams for crack detection International, Journal of Solids and Structures 96:240-253.

Fernández-Sáez, J. and Navarro, C., (2002). Fundamental frequency of cracked beams in bending vibrations: an analytical approach, Journal of Sound and Vibration 256:17-31.

Fernández-Sáez, J., Morassi, A., Pressacco, M., Rubio, L., (2016). Unique determination of a single crack in a uniform simply supported beam in bending vibration, Journal of Sound and Vibration 371:94-109.

Fernández-Sáez, J., Rubio, L., Navarro, C., (1999). Approximate calculation of the fundamental frequency for bending vibrations of cracked beams, Journal of Sound and Vibration 225:345-352.

Gillich, G.R. and Praisach, Z.I., (2014). Modal identification and damage detection in beam-like structures using the power spectrum and time–frequency analysis, Signal Processing 96:29-44.

Gomes, H.M., Almeida, F.J.F., (2014). An analytical dynamic model for single-cracked beams including bending, axial stiffness, rotational inertia, shear deformation and coupling effects, Applied Mathematical Modelling 38:938-948.

Hadjileontiadis, L.J., Douka, E., Trochidis, A., (2005). Fractal dimension analysis for crack identification in beam structures, Mechanical Systems and Signal Processing 19:659-674.

Hou, C., Lu, Y., (2016). Identification of cracks in thick beams with a cracked beam element model. Journal of Sound and Vibration 385:104-124.

Kanaparthi, S., Sekhar, V.R., Badhulika, S., (2016). Flexible, eco-friendly and highly sensitive paper antenna based electromechanical sensor for wireless human motion detection and structural health monitoring, Extreme Mechanics Letter 9:324-330.

Khaji, N. and Mehrjoo, M., (2014). Crack detection in a beam with an arbitrary number of transverse cracks using genetic algorithms, Journal of Mechanical Science and Technology 28:823-836.

Khavita, S., Joseph Daniel, R., Sumangala, K., (2016). High performance MEMS accelerometers for concrete SHM applications and comparison with COTS accelerometers, Mechanical Systems and Signal Processing 66-67:410-424.

Khiem, N.T. and Tran, H.T., (2014). A procedure for multiple crack identification in beam-like structures from natural vibration mode, Journal of Vibration and Control 20:1417-1427.

Krawczuk, M., (1992). Modelling and identification of cracks in truss constructions, Finite Elements in Analysis and Design 12:41-50.

Lee, J., (2009). Identification of multiple cracks in a beam using natural frequencies, Journal of Sound and Vibration 320:482-490.

Loya, J.A., Rubio, L., Fernández-Sáez, J., (2006). Natural frequencies for bending vibrations of Timoshenko cracked beams, Journal of Sound and Vibration 290:640-653.

Lu, X. B., Liu, J. K., Lu, Z. R., (2013). A two-step approach for crack identification in beam. Journal of Sound and Vibration 332:282-293.

Mazanoglu L., Sabuncu, M., (2012). A frequency based algorithm for identification of single and double cracked beams via a statistical approach used in experiment, Mechanical Systems and Signal Processing 30:168-185.

Mehrjoo, M., Khaji, N., Ghafory-Ashtiany, M., (2014). New timoshenko-cracked beam element and crack detection in beam-like structures using genetic algorithm, Inverse Problems in Science and Engineering 22:359-382

Moezi, S.A., Zakeri, E., Zare, A., Nedaei, M., (2015). On the application of modified cuckoo optimization algorithm to the crack detection problem of cantilever Euler–Bernoulli beam, Computers and Structures 157:42-50.

Montanari, L., Spagnoli, A., Basu, B., Broderick, B., (2015). On the effect of spatial sampling in damage detection of cracked beams by continuous wavelet transform, Journal of Sound and Vibration 345:233-249.

Mungla, M.J., Sharma, D.S., Trivedi, R.R., (2016). Identification of a crack in clamped-clamped beam using frequency-based method and genetic algorithm, Procedia Engineering 144:1426-1434. 12th International Conference on Vibration Problems.

Oliveira Filho, M.V.M., Ipiña, J.E.P., Bavastri, C.A., (2017). Analysis of sensor placement in beams for crack identification. MecSol – Proceedings of the 6th International Symposium on Solid Mechanics 536-553.

Owolabi, G.M., Swamidas, A.S.J., Seshadri, R., (2003). Crack detection in beams using changes in frequencies and amplitudes of frequency response functions, Journal of Sound and Vibration 265:1-22.

Rizos, P.F., Aspragathos, N., Dimarogonas, A.D., (1990). Identification of crack location and magnitude in a cantilever beam form the vibration modes, Journal of Sound and Vibration 138:381-388.

Saeed, R.A., Galybin, A.N., Popov, V., (2012). Crack identification in curvilinear beams by using ANN and ANFIS based on natural frequencies and frequency response functions, Neural Computing and Applications 21:1629-1645.

Sankararaman, S., Ling, Y., Mahadevan, S., (2011). Uncertainty quantification and model validation of fatigue crack growth prediction, Engineering Fracture Mechanics 78:1487-1504.

Simoen, E., De Roeck, G., Lombaert, G., (2015). Dealing with uncertainty in model updating for damage assessment: A review, Mechanical Systems and Signal Processing 56-57:123-149.

Srinivasarao, D., Rao, K.M., Raju, G.V., (2010). Crack identification on a beam by vibration measurement and wavelet analysis, International Journal of Engineering Science and Technology 2:907-912.

Xu, Y.F., Zhu, W.D., Liu, J., Shao, Y.M., (2014). Identification of embedded horizontal cracks in beams using measured mode shapes, Journal of Sound and Vibration 333:6273-6294.

Zhang, K. and Yan, X., (2017). Multi-cracks identification method for cantilever beam structure with variable cross-sections based on measured natural frequency changes, Journal of Sound and Vibration 387:53-65.